

RESEARCH ARTICLE

Genes Involved in Organ Separation in Arabidopsis: An Analysis of the *cup-shaped cotyledon* Mutant

Mitsuhiro Aida,¹ Tetsuya Ishida,¹ Hidehiro Fukaki, Hisao Fujisawa, and Masao Tasaka²

Department of Botany, Division of Biological Science, Graduate School of Science, Kyoto University, Kyoto 606-01, Japan

Mutations in *CUC1* and *CUC2* (for *CUP-SHAPED COTYLEDON*), which are newly identified genes of Arabidopsis, caused defects in the separation of cotyledons (embryonic organs), sepals, and stamens (floral organs) as well as in the formation of shoot apical meristems. These defects were most apparent in the double mutant. Phenotypes of the mutants suggest a common mechanism for separating adjacent organs within the same whorl in both embryos and flowers. We cloned the *CUC2* gene and found that the encoded protein was homologous to the petunia NO APICAL MERISTEM (*NAM*) protein, which is thought to act in the development of embryos and flowers.

INTRODUCTION

Development of higher plants is divided into two phases: embryonic and postembryonic. Throughout these phases, new organs and tissues are produced in a set pattern. During embryogenesis, an apical-basal pattern and a radial pattern are established, and organs and tissues of seedlings are arranged on the basis of these patterns (Mayer et al., 1991; Jürgens, 1995). In dicots, two discrete cotyledonary primordia arise symmetrically from an upper surface of the globular embryo, and a shoot apical meristem (SAM) differentiates between these primordia (Mansfield and Briarty, 1991; Barton and Poethig, 1993; West and Harada, 1993). Mutants that affect these structures have been isolated in several species, including Arabidopsis (Mayer et al., 1991; Barton and Poethig, 1993; Jürgens et al., 1994a; Laux et al., 1996) and petunia (Souer et al., 1996).

In Arabidopsis, the *gurke* mutant lacks both cotyledons and a SAM (Mayer et al., 1991), whereas the *laterne* mutant lacks only cotyledons (Mayer et al., 1993). The *shoot meristemless* (*stm*), *zwille*, and *wuschel* mutants lack only a SAM (Barton and Poethig, 1993; Jürgens et al., 1994b; Laux et al., 1996). The *STM* gene encodes a homeodomain protein of the KNOTTED1 class and is thought to be required for the formation and maintenance of the SAM (Long et al., 1996). In petunia, the *no apical meristem* (*nam*) mutant lacks a SAM and has fused cotyledons (Souer et al., 1996). Occasionally, *nam* seedlings produce "escape shoots," some of

which develop into mature plants, but the flowers that are produced by these shoots have various defects, including extra petals and fusion of some organs. These results indicate that the *nam* gene is related to development of both embryos and flowers. The *nam* gene has been cloned, and it encodes a protein of a novel class (Souer et al., 1996).

In postembryonic development, the SAM initially produces vegetative structures, including leaves and stems (Sussex, 1989; Medford, 1992). After the vegetative phase, the SAM is converted into an inflorescence meristem from which floral meristems arise. Floral meristems produce flowers with four types of organs (sepals, petals, stamens, and carpels) arranged in concentric rings or whorls. Several important aspects of flower development, such as determination of meristem and organ identity, are regulated by combinations of transcription factors, including members of the MADS domain family of proteins (Coen and Meyerowitz, 1991; Van der Krol and Chua, 1993; Weigel and Meyerowitz, 1994).

However, how individual primordia develop into discrete organs during both embryonic and postembryonic development is not well understood. Here, we analyze a newly isolated mutant of Arabidopsis, designated *cuc* (for *cup-shaped cotyledon*). The *cuc* mutant showed a fusion of cotyledons (embryonic organs), sepals, and stamens (floral organs) and lacked the embryonic SAM. This phenotype was caused by double mutations at two unlinked loci, *CUC1* and *CUC2*. The phenotype of the *cuc* mutant suggests a common mechanism that regulates separation of organs in both embryo and flower development. One of the *CUC* genes, *CUC2*, was cloned by using transposon tagging.

¹ These authors contributed equally to this work.

² To whom correspondence should be addressed. E-mail tasaka@fuji.bot.kyoto-u.ac.jp; fax 81-75-753-4126.

RESULTS

Isolation and Genetic Analysis of the *cuc* Mutant

We isolated a *cuc* mutant line from descendants of the *chl1-6* (for *chlorate-resistant*) mutant carrying both an endogenous transposon, *Tag1*, and a maize transposon, *Activator* (*Ac*), in a *Landsberg erecta* (*Ler*) background (Tsay et al., 1993). Cotyledons of *cuc* seedlings were fused along the edges of their sides, resulting in a cup-shaped cotyledon (Figure 1B). *cuc* seedlings produced no shoots and eventually died without producing any new organs. The originally isolated mutant line produced ~25% *cuc* seedlings in its selfed progenies (48 of 199 in one experiment). The rest were basically normal (Figure 1A), although a few "heart-type" seedlings were produced. Their cotyledons were fused along one side of their edges (Figure 1C). The extent of fusion varied among different heart-type seedlings. Both normal and heart-type seedlings produced normal shoots.

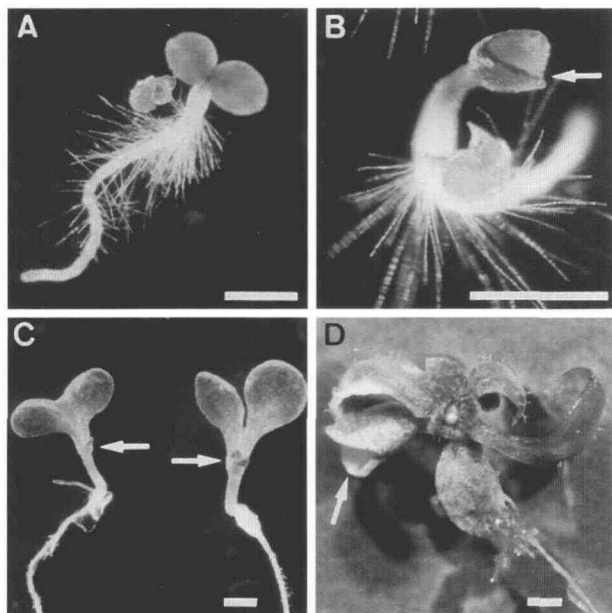


Figure 1. Phenotypes of *cuc* Seedlings.

(A) to (C) Three types of seedlings produced from the original *cuc* mutant line. (A) shows a normal seedling with two separated cotyledons. (B) illustrates a *cuc* seedling with a cup-shaped cotyledon. The upper region of the cup-shaped cotyledon splits in two (arrow). In (C), heart-type seedlings are shown, with arrows indicating developing shoots. The length of the fused part is variable in different heart-type seedlings.

(D) A revertant (line 4) of the *cuc* mutant. An adventitious shoot has emerged from the region of the hypocotyl just below the cup-shaped cotyledon (arrow) and is forming a rosette.

Bars = 1 mm.

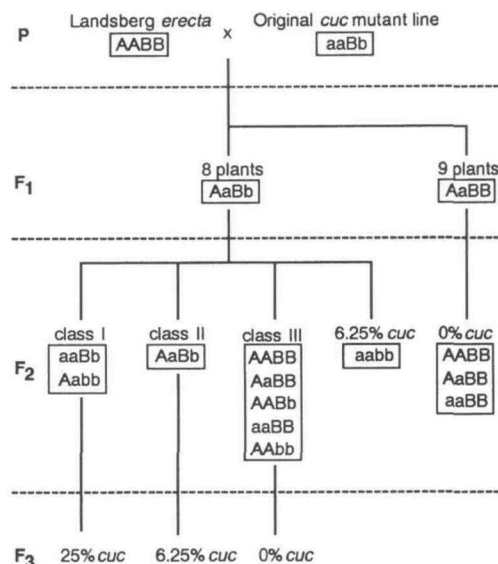


Figure 2. Flow Chart of the Pedigree of the Genetic Analysis.

Predicted genotypes of each plant are represented by combinations of A (for wild-type allele of *CUC1*), a (for mutant allele of *CUC1*), B (for wild-type allele of *CUC2*), and b (for mutant allele of *CUC2*). P, parent.

To determine how many mutations caused the *cuc* phenotype, we backcrossed the original line to wild-type *Ler* (Figure 2). All *F*₁ seedlings were normal. Almost half (eight of 17) of these *F*₁ plants produced ~6.25% (i.e., one-sixteenth) *cuc* seedlings in the *F*₂ generation (Figure 2 and Table 1), whereas the rest produced no *cuc* seedlings (data not shown). One of the *F*₁ lines that produced *cuc* (L103 in Table 1) was subjected to *F*₃ analysis. We grew the *F*₂ siblings of *cuc*, collected their seeds individually, and examined frequencies of *cuc* in the *F*₃ generation. Most of the *F*₂ siblings were divided into three classes, depending on the frequencies of *cuc* (Figure 2 and Table 2). Class I produced ~25%, class II produced ~6.25%, and class III produced no *cuc* seedlings. These results indicate that the *cuc* seedling phenotype is caused by double homozygous mutations at two unlinked loci. The original mutant line was homozygous for one of the mutations and heterozygous for the other, thus producing ~25% *cuc* seedlings in its selfed progenies. The locus with the homozygous mutation in the original line was designated *CUC1*, and the other was designated *CUC2*.

To confirm that the *cuc* phenotype resulted from the action of these two genes, we isolated *cuc1* and *cuc2* single mutant lines from the original mutant line (see Methods) and crossed these lines again. In each single mutant, no *cuc* seedlings were observed, and most of the seedlings were phenotypically normal, except for a few of the seedlings that were of the heart type (Figure 1C; see below). However, all

F₁ plants of the cross between *cuc1* and *cuc2* produced ~6.25% *cuc* seedlings in the F₂ generation (data not shown). These results support that the *cuc* phenotype was caused by double homozygous mutations at the *CUC1* and *CUC2* loci.

Seedling Phenotypes of the *cuc* Mutants

In *cuc1 cuc2* double mutant seedlings (*cuc* seedlings), the upper portion of the cup-shaped cotyledon often split in two (Figure 1B). In addition, the majority of the *cuc* seedlings retained their bilaterally symmetrical shape. Therefore, we speculated that the cup-shaped cotyledon basically consisted of two cotyledons that were fused together. To confirm this, we examined the vascular pattern of wild-type and *cuc* cotyledons.

Figure 3 shows typical vascular patterns of wild-type and *cuc* cotyledons. In the wild type, a midvein runs along the central axis of the cotyledon, and several lateral veins run along its margin (Figure 3A). A small projection marks the distal end of the midvein. In *cuc*, two sets of one midvein (marked by a small projection at the distal end) and two lateral veins were arranged symmetrically on either side of a cup-shaped cotyledon (one of the sides is in focus in Figure 3B). Adjacent lateral veins were connected by another vein (Figures 3B and 3C) or joined at the basal half (data not shown). These observations indicate that a cup-shaped cotyledon essentially consists of two cotyledons.

Figures 4A and 4B show transverse sections of wild-type and *cuc* cotyledons. Wild-type cotyledons had four tissue layers consisting of adaxial epidermis, palisade mesophyll, spongy mesophyll, and abaxial epidermis (Figure 4A). These four tissue layers were also observed in *cuc* cotyledons (Figure 4B), suggesting that the *cuc1 cuc2* double mutations do not affect tissue differentiation of cotyledons.

Histological sections of *cuc* seedlings showed that they completely lacked SAMs. In contrast to wild-type seedlings with SAMs consisting of small, densely stained cells with prominent nuclei (Figure 4C), *cuc* seedlings had large, highly vacuolated cells at the corresponding position (Figure 4D).

Table 1. F₂ Analysis of the *cuc* Mutant

F ₁ Line ^a	Total Number of F ₂ Seedlings	Number of <i>cuc</i> Seedlings	Frequency (%)
L101	268	15	5.6
L103	330	17	5.2
L107	295	18	6.1
L108	368	28	7.6
L109	492	21	4.3
L110	469	27	5.8
L115	459	29	6.3
L117	308	28	9.1

^a F₁ lines that produced *cuc* seedlings in the F₂ generation are shown.

Table 2. F₃ Analysis of the *cuc* Mutant

Class of F ₂ Plants	Number of Plants
I ^a	16
II ^b	15
III ^c	20
IV ^d	1

^a Plants that produced ~25% *cuc* seedlings.

^b Plants that produced ~6.25% *cuc* seedlings.

^c Plants that produced no *cuc* seedlings.

^d A plant that produced 16.8% *cuc* seedlings (50 of 298). This frequency significantly deviates from 25, 6.25, or 0% (P < 0.01), so this plant is excluded from any of the former three classes.

We next examined the phenotype of the *cuc1* and *cuc2* single mutants. Most of the seedlings were normal in both cases, but a few of them were heart-type seedlings whose cotyledons were fused along one side (0.49% for *cuc1* and 0.53% for *cuc2*; Figure 1C). The vascular pattern of a heart-shaped cotyledon in heart-type seedlings indicated that this structure essentially consisted of two cotyledons, because they had two midveins (Figure 3D). A majority of these heart-type seedlings produced normal shoots, indicating the presence of a functional SAM (Figure 1C). In the *cuc2* mutant, however, some of the heart-type seedlings did not produce shoots (two of 13 heart-type seedlings). These heart-type seedlings lacked a SAM (data not shown). Based on these observations, we concluded that the heart-type phenotype could be interpreted as a weaker phenotype of *cuc*. Therefore, the effect of each single mutation on the cotyledon and SAM development is very weak.

The frequency of heart-type seedlings was highest in plants heterozygous for one mutation and homozygous for the other mutation. When *cuc1/cuc1 cuc2/+* plants (i.e., plants homozygous for *cuc1* and heterozygous for *cuc2*) were self-pollinated, 3.6% of the progeny were the heart-type seedlings. Similarly, *cuc1/+ cuc2/cuc2* plants produced 9.2% heart-type seedlings in their selfed progenies. In this case, 11 of 23 heart-type seedlings did not produce shoots.

Embryogenesis of *cuc*

We examined embryogenesis of the *cuc1 cuc2* double mutant (*cuc*) developing in siliques of *cuc1/cuc1 cuc2/+* plants. For the wild type at the globular stage, an embryo consists of a spherical embryo proper and a filamentous suspensor (Figure 5A). The embryo proper has a radially symmetrical shape around the apical-basal axis. The suspensor eventually senesces later in embryogenesis. At the triangular stage, the upper surface of the embryo starts to broaden laterally because of predominant anticlinal divisions of cells in the upper half (Figure 5B). This lateral broadening changes the symmetry of the embryo from radial to bilateral. By the heart

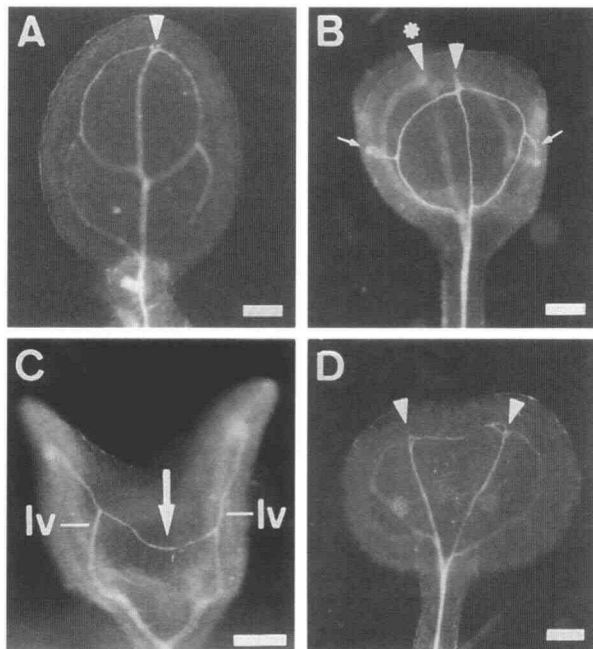


Figure 3. Vascular Patterns of Cotyledons in the Wild Type and *cuc* Mutants.

Seedlings at 2 days after germination were fixed and cleared to visualize vascular strands, as described in Methods.

- (A)** Wild type. An arrowhead indicates the distal end of the midvein.
(B) *cuc*. Vascular strands at one of the sides are in focus. One midvein and two lateral veins are shown, with an arrowhead indicating the distal end of the midvein. The vascular pattern on the opposite side can also be seen, and the distal end of the midvein is indicated by an arrowhead with an asterisk. The veins at both sides are connected by additional veins at lateral sides (small arrows).
(C) Lateral view of the same cotyledon shown in **(B)**. Adjacent lateral veins (lv) are connected by an additional vein (arrow).
(D) Heart type. Arrowheads indicate the distal ends of the midveins.
 Bars = 0.2 mm.

stage, two bulges become apparent in the upper portion and form cotyledonary primordia (Figure 5C). After the heart stage, the cotyledons and hypocotyl elongate to form a torpedo-stage embryo (Figure 5E). Elongation continues, and cotyledons fold over the embryo at the bending cotyledon stage (Figure 5I).

In siliques of *cuc1/cuc1 cuc2/+* plants, no apparently abnormal embryos were observed at the globular stage, suggesting that *cuc* embryos are phenotypically normal until this stage. The difference between the *cuc* mutant and the wild type was first recognized at the heart stage. At this stage, embryos lacking two distinct bulges of cotyledonary primordia were observed (Figure 5D). This type of embryo occupied approximately one-fourth of the heart-stage embryos that were collected from siliques of *cuc1/cuc1 cuc2/+* plants (26.3%; $n = 137$), indicating that these embryos were

cuc. The other embryos were indistinguishable from those of the wild type. The upper region of these *cuc* embryos was narrower than that of the wild type (cf. Figures 5C and 5D). Frequently, a small depression was observed at the center of the upper surface (Figure 5D).

Later at the torpedo stage, the mutant phenotype became more apparent. Figures 5F to 5H show optical sections of a mutant embryo at three different focal planes. These sections reveal that a doughnut-shaped ridge surrounding the apical–basal axis is formed at the upper region of the embryo. The relative length of the ridge was shorter than that of wild-type cotyledons (cf. Figures 5E and 5G). The doughnut-shaped ridge grew further and became cup shaped at the bending cotyledon stage (Figure 5J). These observations indicate that the cup-shaped structure is formed as a fused structure from the early stage of cotyledon development and not by fusion after two separate cotyledons have developed.

In *cuc1/cuc1 cuc2/+* siliques, we also observed embryos in which cotyledonary primordia were fused at one of their sides (heart-type embryos; Figure 5K). The frequency of this type was much lower than that of *cuc* embryos (six of 278 embryos at the torpedo stage). These embryos seem to become heart-type seedlings later.

We next examined the defect in the SAM formation of *cuc* during embryogenesis. In the wild type, the SAM becomes apparent at the bending cotyledon stage. At this stage, the SAM can be observed as a region that broadens and slightly bulges between cotyledons (Figure 4E). Cells in the SAM have large nuclei that occupy most of the cell, whereas the relative size of the nuclei is smaller in the cells outside of the SAM. By contrast, *cuc* embryos at the bending cotyledon stage lacked a SAM at the corresponding region, and both sides of the cup-shaped cotyledon directly met at their bases (Figure 4F). Cells in this region were vacuolating, and the relative size of the nuclei was small, as were the nuclei in the cells around. No dead cells were observed in this region, indicating that the SAM was not lost by cell ablation.

Adventitious SAM Formation of the *cuc* Mutants

To examine the effect of the *cuc* mutations on adventitious SAM formation, hypocotyl explants of the wild type and *cuc1*, *cuc2*, and *cuc1 cuc2* double mutants were grown under conditions promoting shoot regeneration (Table 3). Explants were cultured on callus-inducing medium for 4 days and then transferred onto shoot-inducing medium. After the transfer, most of the explants formed green calli and subsequently formed adventitious shoots. Before shoot formation, calli were indistinguishable among the different genotypes.

Seventeen days after transfer to the shoot-inducing medium, we counted the number of shoots with normally arranged leaves in each genotype (Table 3). The number of shoots per 1 g of calli (fresh weight of tissue) was highest in the wild type, in the middle range in each of the single mutants, and lowest in the double mutant. Longer incubation

on the shoot-inducing medium barely increased the number of shoots in each case. Thus, each single mutation inhibited adventitious SAM formation, and the effect was the most severe in the double mutant.

Phenotypes of the *cuc* Mutants in Postembryonic Development

To examine the effect of the *cuc1 cuc2* double mutations on postembryonic development, we induced shoots from calli derived from hypocotyls of *cuc* seedlings. Regenerated shoots of the double mutants had normal-looking leaves and stems, and their arrangement of flowers on inflorescence stems was essentially the same as that of the wild type (Figures 6A and 6B). Their flowers, however, were abnormal: all sepals and most stamens were severely fused (Figures 6D and 6E, and 7C to 7E), in contrast to wild-type flowers, in which these organs were separated (Figures 6C, 7A, and 7B). Fusion of sepals and stamens was observed in all flowers. Fusion of both medial-to-medial stamens and medial-to-lateral stamens was observed. Some stamens were fused up to the anthers (Figure 7D), and others were fused up to the middle part of the filaments (Figure 7E). In

some cases, stamens were fused to carpels. Petals were frequently lost or undergrown; however, fusion of these organs was not observed. The number of stamens was also frequently reduced. The double mutant flowers produced viable pollen, which was confirmed by pollination (data not shown), but were female sterile.

We next examined flowers of the *cuc1* and *cuc2* single mutant plants that were grown on soil. Their phenotypes were basically identical to each other and were much less severe than those of the double mutant. In each single mutant, sepal fusion was observed in some flowers, although it occurred in only a few sepals and was so slight that it was barely recognizable with the naked eye (Figures 6F and 7F). In individual plants, sepal fusion became more severe in flowers that were produced later, so that both the frequency and extent of the fusion increased. Stamen fusion was also observed occasionally in both single mutant flowers (Figure 6H). Shape and number of petals and fertility of flowers were normal.

Flowers of *cuc1/+ cuc2/cuc2* and *cuc1/cuc1 cuc2/+* plants grown on soil were also examined. In *cuc1/+ cuc2/cuc2* plants, all four sepals were fused in most of the flowers, and the length of the fused part increased when compared with *cuc2* single mutant flowers (Figure 6G). In

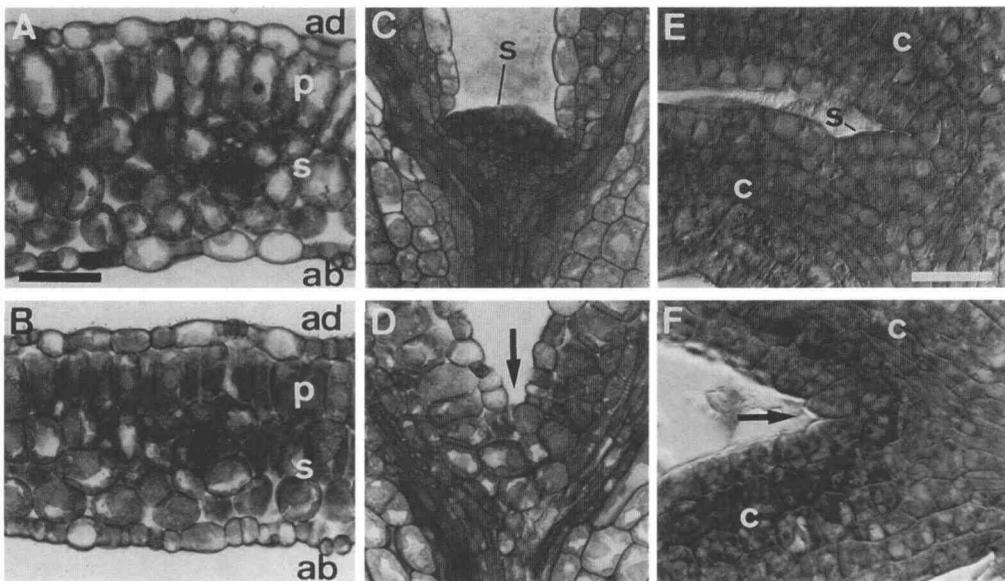


Figure 4. Histological Sections of Wild-Type and *cuc* Seedlings and Embryos.

(A) and (B) Transverse sections of wild-type (A) and *cuc* (B) cotyledons 2 days after germination. The adaxial epidermis (ad), palisade mesophyll (p), spongy mesophyll (s), and abaxial epidermis (ab) are present in both wild-type and *cuc* cotyledons.

(C) and (D) Apices of wild-type (C) and *cuc* (D) seedlings 2 days after germination. Median longitudinal sections are shown. The SAM (s) is present between the cotyledons in the wild type, whereas no SAM is present in *cuc* cotyledons at the corresponding position (arrow).

(E) and (F) Apices of wild-type (E) and *cuc* (F) embryos at the bending cotyledon stage. Median longitudinal sections were viewed with Nomarski (Nikon, Tokyo, Japan) optics. The bases of the cotyledons are separated by the SAM (s) in the wild type, whereas both sides of the cup-shaped cotyledon meet directly at their bases (arrow). c, cotyledon.

Bar in (A) = 50 μ m for (A) to (D); bar in (E) = 20 μ m for (E) and (F).

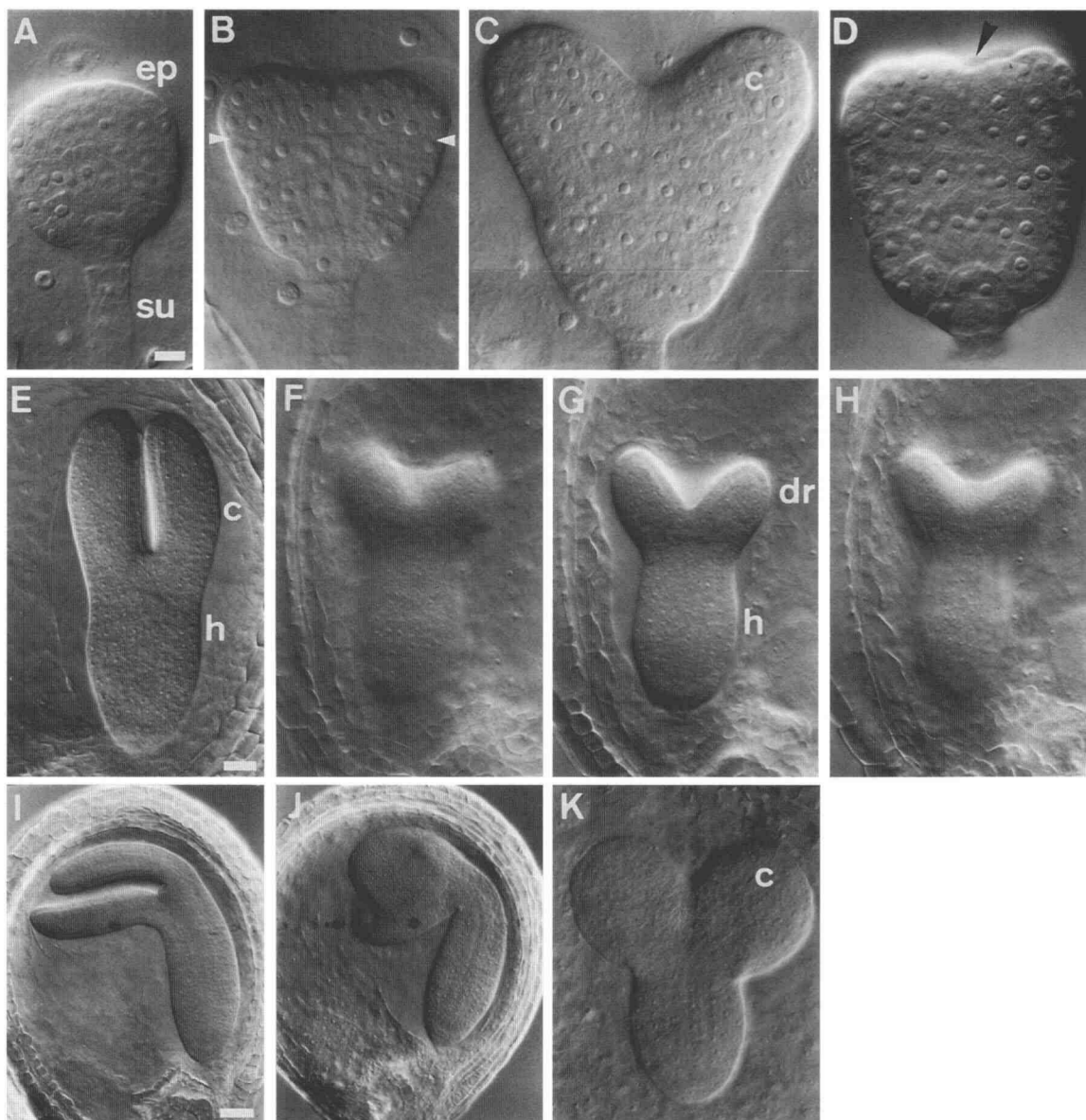


Figure 5. Embryogenesis of the Wild Type and *cuc* Mutants.

Developing embryos were visualized by clearing ovules, as described in Methods, and were viewed with Nomarski optics.

(A) Wild-type embryo at the globular stage.

(B) Wild-type embryo at the triangular stage. Arrowheads indicate the boundary between the upper and lower half of the embryo.

(C) Wild-type embryo at the heart stage.

(D) *cuc* embryo at the heart stage. An arrowhead indicates a small depression at the center of the upper surface.

(E) Wild-type embryo at the torpedo stage.

(F) to (H) *cuc* embryo at the torpedo stage at three different focal planes. The medial plane is shown in **(G)**.

(I) Wild-type embryo at the bending cotyledon stage.

(J) *cuc* embryo at the bending cotyledon stage.

(K) Heart-type embryo in which cotyledonary primordia are fused along one of their sides.

c, cotyledonary primordium; dr, doughnut-shaped ridge; ep, embryo proper; h, hypocotyl; su, suspensor.

Bar in **(A)** = 8 μ m for **(A)** to **(D)**; bar in **(E)** = 20 μ m for **(E)** to **(H)** and **(K)**; bar in **(I)** = 40 μ m for **(I)** and **(J)**.

Table 3. Efficiencies of Shoot Regeneration

Genotype	Number of Shoots ^{a,b}	Fresh Weight (g) ^c	Number of Shoots per 1 g of Calli
<i>Ler</i>	110	1.108	99.3
<i>cuc1</i>	47	1.171	40.1
<i>cuc2</i>	83	1.702	48.8
<i>cuc1 cuc2</i>	10	0.813	12.3

^aFor each genotype, shoot numbers of 10 calli that were grown for 17 days after transfer to shoot-inducing medium were counted.

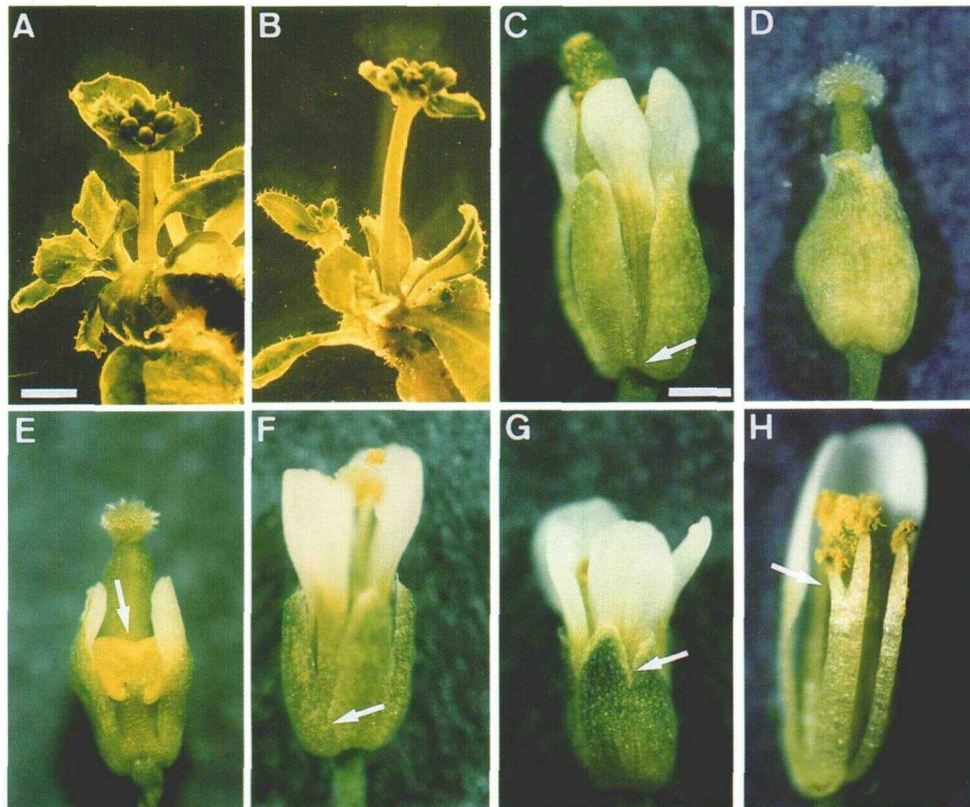
^bA shoot is defined as a structure in which more than two leaves or leaflike structures are spirally arranged around one point of a callus.

^cMeasured on the same day in which the number of shoots was counted.

addition, the fertility of *cuc1/+ cuc2/cuc2* flowers was poor compared with that of the wild type. These observations suggest that the severity of sepal fusion in the *cuc2* single mutant is increased by *cuc1* heterozygosity. *cuc1/cuc1 cuc2/+* flowers showed a phenotype almost identical to that of *cuc1/+ cuc2/cuc2* flowers (Figure 7G), except that their fertility was normal, suggesting that the severity of sepal fusion in the *cuc1* single mutant was also increased by *cuc2* heterozygosity.

Flower Development of *cuc*

To determine how the fusion of sepals and stamens occurs, we compared floral development of the *cuc1 cuc2* double mutant (*cuc*) with that of the wild type. Similar to the wild type, mutant flowers developed four discrete sepal primordia

**Figure 6.** Phenotypes of *cuc* Mutants during Postembryonic Development.

(A) and (B) Shoots regenerated from wild-type (A) and *cuc* mutant (B) calli.

(C) Wild-type flower. Sepals are separated from the basalmost part (arrow).

(D) and (E) *cuc1 cuc2* double mutant flower. A part of the fused sepals in (E) was removed to show the fused stamens (arrow).

(F) and (G) *cuc2* single mutant (F) and *cuc1/+ cuc2/cuc2* (G) flowers. Arrows indicate the uppermost points of the fused parts.

(H) *cuc1* single mutant flower. The sepals and petals in the front were removed to show the fused stamens (arrow).

Bar in (A) = 5 mm for (A) and (B); bar in (C) = 1 mm for (C) to (H).

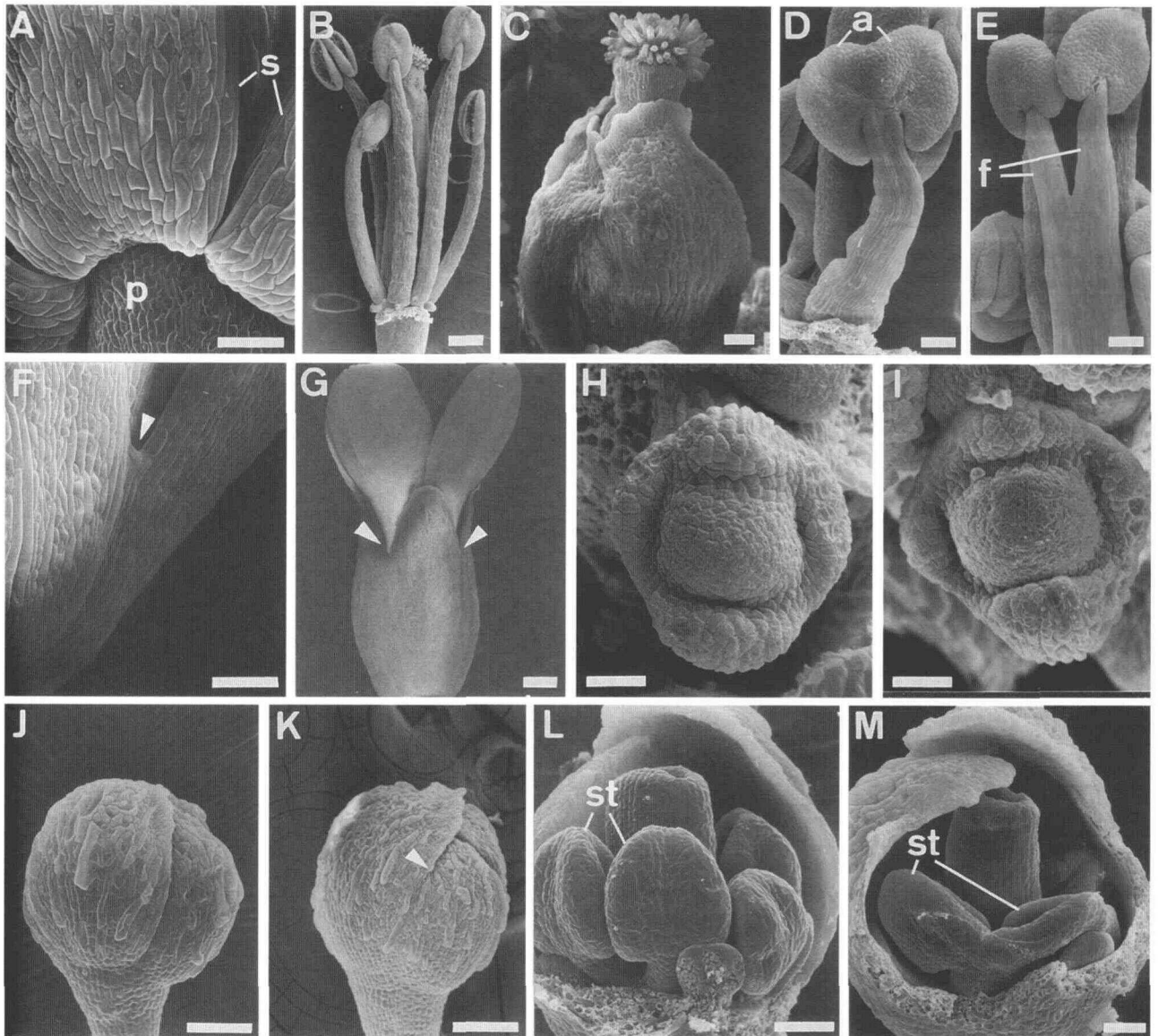


Figure 7. Morphology and Development of *cuc* Mutant Flowers.

(A) Mature wild-type flower. A part of the sepals (s) just above the pedicel (p) is shown. Bar = 100 μ m.

(B) Stamens of a mature wild-type flower. Sepals and petals were removed. Bar = 250 μ m.

(C) Mature *cuc1 cuc2* double mutant flower. Bar = 100 μ m.

(D) and **(E)** Fused stamens of *cuc1 cuc2* double mutant flowers. Stamens are fused up to the middle part of the anthers (a) in **(D)** and up to the middle part of filaments (f) in **(E)**. Bars = 100 μ m.

(F) and **(G)** Sepals of mature flowers of the *cuc1* single mutant **(F)** and *cuc1/cuc1 cuc2/+* heterozygote **(G)**, with arrowheads indicating the uppermost points of the fused parts. Bar in **(F)** = 100 μ m; bar in **(G)** = 250 μ m.

(H) and **(I)** Flowers of the wild type **(H)** and *cuc1 cuc2* double mutant **(I)** at stage 4. Bars = 20 μ m.

(J) and **(K)** Flowers of the wild type **(J)** and *cuc1 cuc2* double mutant **(K)** at stage 8. An arrowhead in **(K)** indicates the uppermost point of the fused part. Bars = 100 μ m.

(L) and **(M)** Flowers of the wild type **(L)** and the *cuc1 cuc2* double mutant **(M)** at stage 9. Sepals were removed to show stamen primordia (st). Bars = 50 μ m.

at symmetrical positions (Figures 7H and 7I). No difference was observed between *cuc* and the wild type until four sepals enclosed buds. These observations indicate that the *cuc1 cuc2* double mutations do not alter the number or positions of sepal primordia.

Afterward, sepals continued to develop separately in the wild type, and medial sepals covered the margins of lateral sepals (Figure 7J). By contrast, adjacent sepals of *cuc* were fused together in more basal regions, forming a continuous structure (Figure 7K). Figures 7L and 7M show developing stamen primordia of the wild type and *cuc*. In contrast to the wild type, in which stamen primordia were developing separately (Figure 7L), stamen primordia of *cuc* were fused in more basal regions (Figure 7M). These observations indicate that fused sepals and stamens of *cuc* develop as fused structures from early stages of their formation.

The *CUC2* Gene Was Tagged by *Tag1*

Because the *cuc* mutant was isolated from the *chl1-6* line containing both *Tag1* and *Ac* (Tsay et al., 1993), it was expected that at least one of the *CUC* genes would be tagged by either of the transposons. To examine this possibility, genomic DNAs were isolated from *cuc1/cuc1* *+/+* and *cuc1/cuc1 cuc2/+* plants, and DNA gel blot hybridization using a part of *Tag1* or *Ac* sequences as a probe was performed. Polymorphisms were observed only when blots were probed with the *Tag1* fragment (data not shown), suggesting that the *cuc2* mutation was caused by *Tag1* insertion.

In general, when a mutation is caused by insertion of a transposon, revertants are obtained with excision of the transposon. To date, four tentative revertants were obtained from ~10,000 *cuc* seedlings. Each revertant generated an adventitious shoot at the region of the hypocotyl just below the cup-shaped cotyledon (Figure 1D) and formed a fertile plant. In their selfed progenies, ~25% of seedlings produced were *cuc*. DNA gel blot analysis showed that a 2.1-kb *cuc2*-specific band probed with the *Tag1* fragment disappeared with all four reversions and that a new band specific to a reversion appeared in one revertant line (Figure 8, line 1). On the other hand, no polymorphisms were observed using an *Ac* fragment as a probe (data not shown). These results indicate that the *cuc2* mutation is caused by *Tag1* insertion. The *Ac* element segregated from the *cuc* mutant phenotype after the backcross, indicating that either the *cuc1* or *cuc2* mutation is not linked to *Ac*.

Cloning and Structure of *CUC2*

A 400-bp genomic fragment flanking to the *Tag1* was amplified by conducting inverse polymerase chain reaction (PCR), using the 2.1-kb *cuc2*-specific fragment. Using this 400-bp product as a probe, we isolated 11 genomic DNA clones from a λ library made from wild-type genomic DNA (Columbia

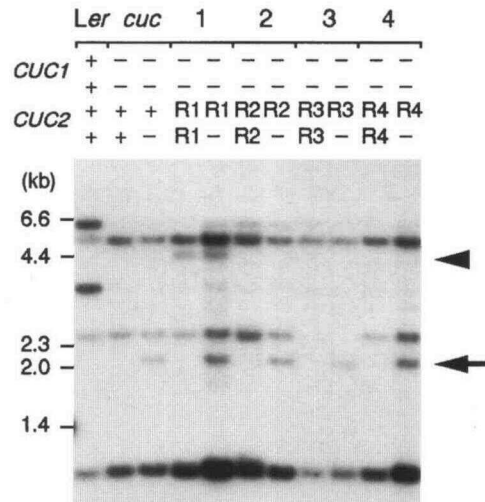


Figure 8. Genomic DNA Gel Blot Analysis.

Genomic DNAs digested with *Bgl*III were probed with the *Tag1* fragment. Genomic DNAs were extracted from the following lines: the wild type (*Ler*), the original mutant line (*cuc*), and four revertant lines (1 to 4). Genotypes of each plant were represented by a combination of + (wild-type allele), - (mutant allele), and R1 to R4 (revertant alleles). The arrow indicates a 2.1-kb *cuc2*-specific band. The arrowhead indicates a new band that is specific to the reversion. DNA length markers are given at left in kilobases.

ecotype). All 11 clones included the same sequence to the 400-bp PCR product. From these 11 clones, a 3.4-kb sequence that contained the identical sequence to the 400-bp product was determined.

The 3.4-kb sequence contained a region significantly homologous to the petunia *nam* gene (see below; Souer et al., 1996). In addition, the phenotype of the *cuc* mutant was similar to that of the *nam* mutant. From these results, we concluded that the 3.4-kb sequence contained the *CUC2* gene. Although screenings for *CUC2* cDNA were unsuccessful, sequence comparison of the 3.4-kb sequence to the *nam* gene showed the exon-intron structure of the *CUC2* gene and the deduced amino acid sequence of the *CUC2* protein (Figure 9). The predicted *CUC2* protein is a 375-amino acid polypeptide and has an apparent molecular mass of 41.4 kD. To confirm that the *cuc2* mutation was caused by *Tag1* insertion, genomic regions around termini of the *Tag1* were amplified from genomic DNA of a plant line heterozygous for *cuc2*. Comparisons of these genomic regions and the 3.4-kb sequence revealed that 8 bp of genomic DNA was duplicated at the *Tag1* insertion site. The insertion site is 19 bp downstream from a putative translation start point (Figure 9A), indicating that the *cuc2* mutation is a loss-of-function mutation and that this allele does not produce a functional protein. In all four revertants, each *Tag1* element had been excised without any footprints (data not shown).

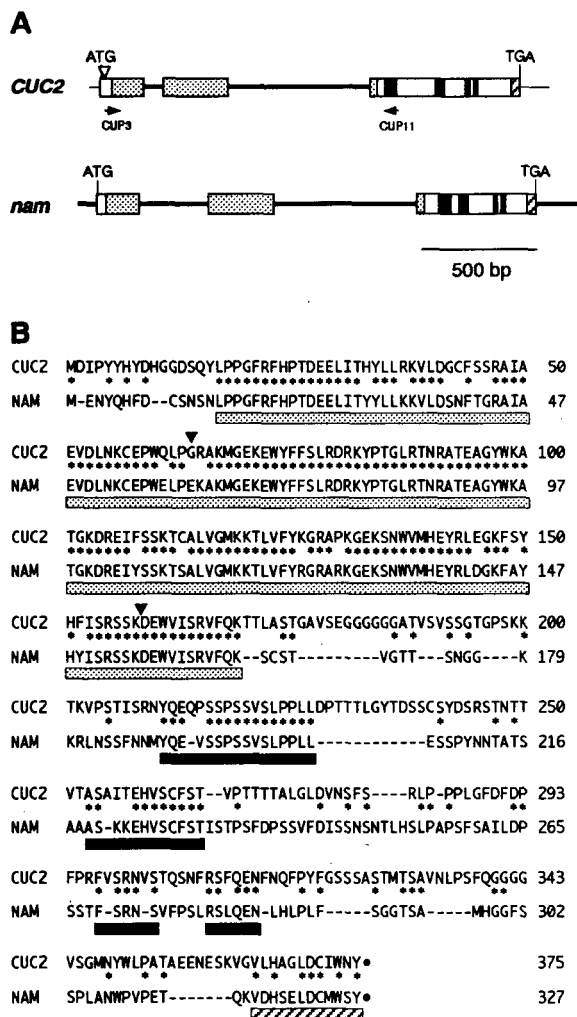


Figure 9. Comparison of the Genomic Organization and Amino Acid Sequences of *CUC2* and *nam*.

(A) The exon-intron structure of *CUC2* and *nam*. Introns and untranslated regions are indicated by thick lines. Exons are indicated by boxes. Various boxes represent homologous amino acid regions: stippled boxes represent the NAC domain, filled boxes represent serine-rich regions, and hatched boxes represent C-terminal regions. The 5' and 3' untranslated regions of *CUC2* have not yet been determined. The open triangle indicates the *Tag1* insertion site. PCR primers CUP3 and CUP11 used for RT-PCR are indicated below the *CUC2* map.

(B) Comparison of the amino acid sequences of *CUC2* and *NAM*. Asterisks indicate identical amino acids in both sequences. A NAC domain is underlined with a stippled bar, serine-rich regions are indicated with filled bars, and a C-terminal region is underlined with a hatched bar. Intron positions are indicated by filled triangles. Hyphens and filled circles indicate gaps in the sequence and stop codons, respectively.

Homology of *CUC2* to Other Genes

When we used the *CUC2* DNA sequence to search the available databases, the petunia *nam* gene and several cDNA clones of Arabidopsis and rice were found to contain sequences significantly homologous to the region encoding the N-terminal part of the *CUC2* protein. Most of these sequences were expressed sequence tags, except for *nam* and two Arabidopsis clones, ATAF1 and ATAF2. The *NAM* protein, ATAF1, and ATAF2 were 56.0, 35.3, and 32.3% identical, respectively, to the predicted *CUC2* protein. In addition, they were 89.5, 58.1, and 55.1% identical, respectively, to the *CUC2* protein in the N-terminal region (from positions 17 to 169) (Table 4). We named this conserved N-terminal region the NAC domain (for petunia *NAM* and Arabidopsis *ATAF1*, *ATAF2*, and *CUC2*). Proteins containing the NAC domain would be members of a gene family encoding a novel type of proteins. This gene family can be divided into at least two subfamilies based on amino acid sequence similarities within the NAC domain: one is represented by *CUC2* and *NAM* and the other by *ATAF1* and *ATAF2*.

Regions of homology between *CUC2* and *NAM* were not only the NAC domain but also five short regions: four serine-rich regions and the C-terminal region (Figure 9B). In the predicted *CUC2* protein, however, none of the known amino acid sequence motifs or signal peptide sequences could be detected.

Expression of the *CUC2* Gene

From the phenotype of the *cuc1 cuc2* double mutant, we hypothesized that the *CUC2* gene would be expressed during embryogenesis and floral organogenesis. *CUC2* transcripts were detected on gel blot of poly(A)⁺ RNA from buds but not from the aerial part of seedlings (Figure 10A). To examine the expression in detail, reverse transcriptase-PCR (RT-PCR) was used to detect the transcript (Figure 10B).

The PCR primer sequences CUP3 and CUP11 were located in the first and third exons, respectively (Figure 9A). The sequence of the PCR product was identical to a corresponding sequence of the predicted *CUC2* cDNA. The product was amplified significantly from bud and flower RNAs, minimally from the aerial parts of seedling, inflorescence, and old silique RNAs, and barely or not at all from RNAs of other tissues (Figure 10B).

Table 4. Comparison of Amino Acid Identities within the NAC Domain

	<i>NAM</i> (%)	<i>ATAF1</i> (%)	<i>ATAF2</i> (%)
<i>CUC2</i>	89.5	58.1	55.1
<i>NAM</i>	—	56.1	54.5
<i>ATAF1</i>	—	—	83.7

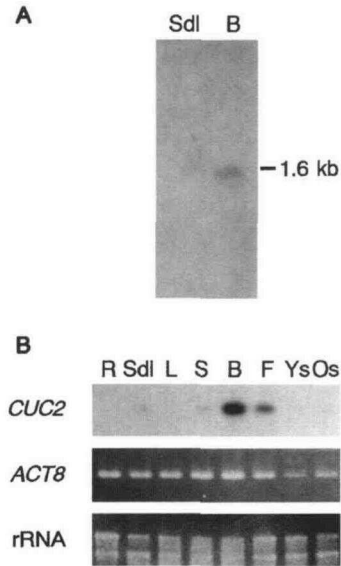


Figure 10. Expression of *CUC2*.

(A) RNA gel blot analysis. A DNA fragment corresponding to the third exon of *CUC2* was labeled and reacted with a poly(A)⁺ RNA gel blot. The number at right indicates the approximate length of the mRNA detected.

(B) Expression of *CUC2* mRNA detected by using RT-PCR. RT-PCR products were diluted 1000-fold, and 10 μL of the diluted products was electrophoresed on an agarose gel, transferred to nylon membranes, and hybridized with a *CUC2* probe. The *CUC2* probe in this experiment was the RT-PCR product from floral bud clusters (top). As an internal control, expression of the *ACT8* mRNA was detected using RT-PCR. RT-PCR products were electrophoresed on an agarose gel and stained with ethidium bromide (middle). As a control, 18S and 28S rRNAs, which were included in each total RNA in the same volumes as those used for RT-PCR, were also electrophoresed on an agarose gel and stained with ethidium bromide (bottom). R, roots of 7-day-old seedlings; Sdl, aerial parts of 7-day-old seedlings; L, mature rosette leaves; S, inflorescence stems; B, bud clusters, including inflorescence meristems; F, open flowers; Ys, young siliques containing developing embryos (from zygotes to torpedo-stage embryos); Os, old siliques containing maturing embryos (from torpedo-stage to mature embryos).

Linkage Analysis of the *CUC1* and *CUC2* Loci

To determine chromosomal locations of the *CUC1* and *CUC2* loci, we performed linkage analyses. Flowers of plants of the Columbia ecotype were pollinated with pollen from *cuc1 cuc2* double mutant flowers, which were obtained by shoot regeneration. Genomic DNAs of F₂ *cuc* seedlings were examined for linkage to five simple sequence length polymorphism (SSLP) markers (Bell and Ecker, 1994). The data shown in Table 5 indicate that *CUC1* and *CUC2* are located on chromosomes 3 and 5. At the same time, the *cuc* mutant line was crossed to CS3078 plants, which carried *tt3*, a visible marker on chromosome 5. Of the 83 F₂ *cuc* seedlings, only five showed *tt3* phenotype (seedlings homozygous for the *tt3* mutation were recognized by their lack of anthocyanin production). This ratio significantly deviates if independent inheritance of the *tt3* and either of the *cuc* mutations is assumed ($P < 0.001$; chi square test), supporting that one of the *CUC* loci is on chromosome 5.

To determine the chromosomal location of *CUC2*, we performed another linkage analysis. By using PCR primers that could detect a polymorphism between the wild-type and mutant alleles of *CUC2*, plants homozygous for wild-type *CUC2* were selected from the F₂ progenies derived from a cross between wild-type Columbia and the double mutant plants. Genomic DNA of these plants was analyzed with SSLP and cleaved amplified polymorphic sequence (CAPS) markers (Konieczny and Ausubel, 1993). No linkage was detected to *nga162*, which is on chromosome 3 (data not shown). On the other hand, a significant linkage to *LFY3*, a CAPS marker on chromosome 5, was detected (Table 5). These results indicate that *CUC2* is on chromosome 5, and therefore, *CUC1* is on chromosome 3.

DISCUSSION

We isolated the novel seedling lethal mutant of Arabidopsis, *cuc*, and showed that the phenotype of this mutant was caused by double mutations at two unlinked loci, *CUC1* and

Table 5. Linkage Analyses of the *CUC* Loci

Marker (Linkage Group)	Total Number of Chromosomes Examined	Recombination Events	Recombination Frequency (% ± SE)
<i>nga280</i> ^a (1)	54	31	57.4 ± 6.7
<i>nga168</i> ^a (2)	36	23	63.8 ± 8.0
<i>nga162</i> ^a (3)	48	3	6.3 ± 3.5
<i>nga8</i> ^a (4)	50	29	58.0 ± 7.0
<i>nga76</i> ^a (5)	46	17	37.0 ± 7.1
<i>LFY3</i> ^b (5)	54	5	9.3 ± 3.9

^a Data obtained from *cuc* seedlings in the F₂ generation of the cross between Columbia and the *cuc1 cuc2* double mutant plants.

^b Data obtained from plants homozygous for the wild-type *CUC2* allele in the F₂ generation of the cross between Columbia and the *cuc1 cuc2* double mutant plants.

























Genotype		Seedling	SAM		Flower		
<i>CUC1</i>	<i>CUC2</i>	Cotyledon	Embryonic	Adventitious	Sepal fusion	Stamen fusion	Reduction of petal and stamen number
+/+	+/+	normal 	+	+++	- 	- 	-
+/-	+/+	n.d.	+	n.d.	very weak 	+ 	-
+/+	+/-	n.d.	+	n.d.	very weak 	+ 	-
+/-	+/-	n.d.	+	n.d.	weak 	+ 	-
-/-	+/+	normal and heart (0.49%) 	+	++	weak 	+ 	-
+/+	-/-	normal and heart (0.53%) 	+/-	++	weak 	+ 	-
-/-	+/-	normal and heart (3.6%) 	+	n.d.	intermediate 	+ 	-
+/-	-/-	normal and heart (9.2%) 	+/-	n.d.	intermediate 	+ 	-
-/-	-/-	cup-shaped 	-	+	strong 	++ 	+

Figure 11. Summary of Phenotypes of *cuc* Mutants.

Phenotypes of *cuc* mutants in all possible genotypes of *CUC1* and *CUC2* are shown with schematic diagrams of seedlings, sepals, and stamens. Genotypes are given in combinations of + (for wild-type alleles) and - (for mutant alleles). In the column providing seedling phenotypes, percentages of heart-type seedlings are shown within parentheses. Phenotypes of the embryonic SAMs are represented by + (the SAM is present), - (the SAM is absent), and +/- (some of the heart-type seedlings lack a SAM). Efficiencies of adventitious SAM formation in shoot regeneration are represented by +++ (high efficiency), ++ (intermediate efficiency), and + (low efficiency). The relative strength of the sepal fusion phenotype was determined based on frequencies of fusion events per flower and lengths of fused parts. Phenotypes of the stamen fusion are represented by - (basically separated), + (some of the stamens are fused at low frequencies), and ++ (most of the stamens are fused). Phenotypes of petal and stamen number are represented by - (not reduced) and + (reduced). n.d., not determined.

CUC2. Phenotypes in all possible combinations of *CUC1* and *CUC2* alleles are summarized in Figure 11. The *cuc1* and *cuc2* mutations caused the fusion of cotyledons, sepals, and stamens and impaired the formation of both embryonic and adventitious SAMs. These defects were most apparent in the *cuc1 cuc2* double mutant. The phenotype of the mutants suggests a mechanism that separates organs developing at adjacent positions. The regulation of the organ separation may be crucial for plants to attain their final form.

The *cuc* Mutations Impair Separation of Both Embryonic and Floral Organs

Cotyledons of *cuc* seedlings were fused along the edges of both of their sides, resulting in a cup-shaped cotyledon. Overall morphology, vascular pattern, and tissue organization of this structure indicate that it essentially consists of two normally differentiated cotyledons. Thus, the *cuc1 cuc2* double mutations most likely impair the separation of cotyledons without altering their number or positions. Cotyledons of dicots, including Arabidopsis, are initiated as two discrete bulges during the transition from the globular to heart stage of

embryogenesis (Figures 5A to 5C; West and Harada, 1993). They then grow by regulated cell division and elongation and are kept separated throughout their development. The *cuc1 cuc2* double mutations may have caused fusion by altering the regulation of cell division during embryogenesis. Alternatively, the double mutations may have caused fusion after two cotyledons had already formed. Our observations indicate that the cup-shaped cotyledon of the *cuc* mutant develops as a fused structure from the beginning of cotyledon development, supporting the former interpretation.

Although *cuc* seedlings stopped further development because of the lack of a SAM, we could examine the effect of the double mutations on postembryonic development by shoot regeneration. Regenerated double mutant shoots had flowers with severely fused organs. In most cases, fusion occurred between organs within the same whorls (between sepals and between stamens). These fused organs developed as fused structures from early stages of organogenesis. Thus, the *cuc* mutations impair separation of not only cotyledons but also sepal and stamens.

The patterns of cotyledon and floral organ development are similar in that the same type of primordia are produced almost at the same time in a whorled manner (for details of

cotyledon development, see West and Harada [1993]; for flower development, see Smyth et al. [1990]). Therefore, a common mechanism would function to separate adjacent primordia in the same "whorl" during embryogenesis and flower development. A model for such an organ separation mechanism is presented in Figure 12. In Arabidopsis, sepals, petals, stamens, and, of course, cotyledons are separated. In contrast to these separated organs, two carpels are fused together to make up a gynoecium. In our model, we hypothesize that the separation mechanism acts in the regions between organs of an outer whorl of embryos (i.e., a ring-shaped zone where cotyledons develop) and of whorls 1 to 3 of flowers, but not in those of whorl 4. Both *CUC1* and *CUC2* seem to be involved in the separation mechanism in the outer whorl of embryos and whorls 1 and 3 of flowers, as is suggested from the mutant phenotypes. There may be another gene(s) involved in the organ separation in whorl 2. If so, a "sympetalous" mutant (i.e., a mutant with flowers in which petals are fused) of Arabidopsis may be isolated in the future.

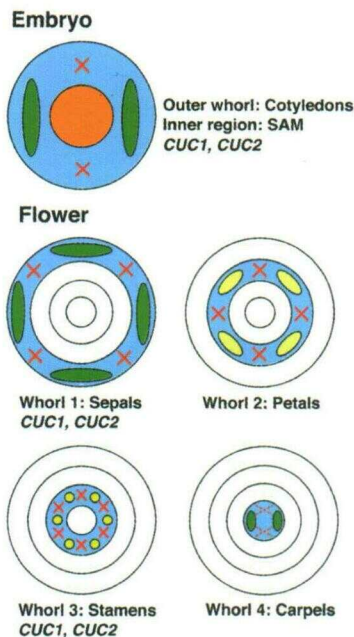


Figure 12. A Model for Organ Separation in Arabidopsis.

X's represent the activity of the organ separation mechanism working in the regions between adjacent organs (represented by ovals) in the same whorls (represented by blue circles). Dotted X's represent the absence of this activity in whorl 4, because two carpels are fused in wild-type Arabidopsis. An orange circle represents the region in which the embryonic SAM develops. *CUC1* and *CUC2* are involved in the separation of organs in the outer whorl of the embryo and in whorls 1 and 3 of the flower as well as in the formation of the SAM in the embryo.

The *cuc* Mutations Impaired Both Embryonic and Adventitious SAM Formation

The *cuc1 cuc2* double mutations completely blocked embryonic SAM formation and also partly inhibited adventitious SAM formation during shoot regeneration from calli. Each single mutation also inhibited adventitious SAM formation. These results suggest that the *CUC* genes are involved in SAM formation both in embryogenesis and shoot regeneration.

Adventitious shoots regenerated from double mutant calli produced leaves and stems, and finally, inflorescences. This result indicates that even in the double mutant, the SAM maintains its activity to form new organs and tissues after it has been formed. The shape of leaves and stems and the pattern of inflorescences are normal in the double mutant, suggesting that the *CUC* genes are not involved in formation of these structures.

The *CUC2* Gene Is a Member of a Gene Family with a Conserved NAC Domain

We cloned one of the *CUC* genes, *CUC2*, by using transposon tagging. The *CUC2* protein belongs to a protein family that includes petunia NAM and several other proteins of Arabidopsis and rice. They share a highly conserved N-terminal domain, which was designated the NAC domain. We found no homologous genes of animals or yeast sequences in the databases. This gene family can be divided into at least two subfamilies based on similarities within the NAC domain: one includes *CUC2* and NAM, and the other includes ATAF1 and ATAF2. The *CUC2* protein does not have any of the known amino acid sequence motifs or signal peptide sequences, so the function of this protein remains to be determined.

Both the *CUC2* and *nam* genes would have important roles in embryogenesis and flower development. In embryogenesis, mutations in these two genes cause similar phenotypes. In *nam*, most of the seedlings lack a SAM and have cotyledons that are fused along one of their sides (Souer et al., 1996). Similarly, a fraction of *cuc2* single mutants shows fusion of cotyledons in one of their sides, and some of them lack a SAM and do not produce shoots (heart-type seedlings; Figures 1C and 11). However, the penetrance of each mutation is very different: most *cuc2* seedlings are normal, in contrast to the *nam* mutant, in which most seedlings are abnormal. Because the sequence analysis of the *cuc2* mutant suggests that this allele does not produce a functional protein, the incomplete penetrance of the *cuc2* mutation can be explained by functional redundancy between the *CUC1* and *CUC2* genes (discussed below).

In flower development, by contrast, the phenotypes of *cuc2* and *nam* are different. For example, emergence of extra organs, which is observed in the *nam* mutant, is not seen in the *cuc2* mutant. Furthermore, the *nam* mutation mainly affects petal formation, whereas the *cuc2* mutation affects sepal and stamen formation. These phenotypic differences

suggest that the *CUC2* and *nam* genes have different functional roles in flower development. Alternatively, these two genes may have the same function, and the phenotypic differences may be due to difference of genetic backgrounds between *Arabidopsis* and *petunia*.

Expression Pattern of *CUC2*

From the phenotypes of the *cuc* mutants, it was expected that *CUC2* is expressed during embryogenesis and floral organogenesis. The gel blot analyses of poly(A)⁺ RNA and RT-PCR revealed that *CUC2* was expressed mainly during floral organogenesis. However, the *CUC2* transcripts were barely detectable from young siliques containing developing embryos. We could not detect these transcripts, possibly because the ratio of the *CUC2* transcripts in total RNA may have been reduced. This may be the result of embryos being part of the silique or of limited expression of *CUC2* both spatially and temporally. Although the analysis with RT-PCR revealed that *CUC2* was weakly expressed in aerial parts of seedling and inflorescence, the *CUC2* gene may not be important for maintenance of the SAM or formation of inflorescence, which was suggested by the analysis of regenerated shoots of *cuc*.

To elucidate the role of *CUC2*, it is necessary to analyze its expression in detail. Analyses of mRNA expression via in situ hybridization and transgenic plants harboring chimeric constructs consisting of the *CUC2* promoter fused to β -glucuronidase and green fluorescent protein reporter genes are in progress. Analysis of protein expression by using anti-*CUC2* antibodies is also in progress.

CUC1 and *CUC2* Are Functionally Redundant

Effects of each single mutation were very similar and slight both in seedlings and flowers but were synergistically enhanced when they were combined in the double mutant. In addition, the severity of each single mutant phenotype in seedlings and flowers was enhanced when heterozygosity of the other mutation was added. These results suggest that the *CUC1* and *CUC2* genes are functionally redundant, and activity of one gene can partly compensate for the loss of the other gene's activity. They also suggest that activity of these genes is dose dependent. Many examples of genetic redundancy are known both in plants and animals (Thomas, 1993; Pickett and Meeks-Wagner, 1995). In *Arabidopsis*, for example, the *cauliflower* (*cal*) mutant displays no phenotype in the single mutant, but it displays a phenotype in the *apetala1* (*ap1*) mutant background (Bowman et al., 1993). This result indicates that the *AP1* and *CAL* genes are functionally redundant and that *AP1* activity can completely compensate for *CAL* gene activity. Both *AP1* and *CAL* genes encode MADS domain proteins and share high similarity to each other (Mandel et al., 1992; Kempin et al.,

1995). It is also possible that *CUC1* encodes a protein similar to *CUC2*.

METHODS

Plant Growth Conditions and Plant Strains

Plants were soil grown at 23°C under constant white light as described by Fukaki et al. (1996a). *Arabidopsis thaliana* ecotype Landsberg *erecta* (*Ler*) was used as the wild type unless otherwise noted. The *chl1-6* mutant line was kindly provided by N.M. Crawford (University of California, La Jolla) and C. Dean (John Innes Centre, Norwich, UK). The CS3078 mapping line used for linkage analysis was kindly provided by the *Arabidopsis* Biological Resource Center (Ohio State University, Columbus).

Analysis of Seedling Phenotypes

For analyses of seedling phenotypes, we surface sterilized seeds and sowed them on Murashige and Skoog plates containing Murashige and Skoog salts (Wako Pure Chemical Industries, Ltd., Osaka, Japan), as described by Fukaki et al. (1996b). After incubation for at least 3 days at 4°C in darkness, plates were incubated in a growth chamber at 23°C under constant white light.

Isolation of *cuc1* and *cuc2* Single Mutant Lines

The original *cuc* mutant line was backcrossed three times to *Ler*. Among the F₂ progenies of the third backcross, several lines (13, 15, 18, 19, and 20) that produced ~25% *cuc* seedlings were isolated and examined for the genotype of the *CUC2* locus, using polymerase chain reaction (PCR) primers that could detect a polymorphism between the wild-type and mutant alleles of *CUC2*. Line 20 was homozygous and the others were heterozygous for the *cuc2* mutation, indicating that the genotype of line 20 was *cuc1/+ cuc2/cuc2* and that the other lines were *cuc1/cuc1 cuc2/+*. Putative *cuc1* and *cuc2* single mutants were isolated from selfed progenies of lines 18 and 20, respectively. At the same time, a *cuc1* single mutant line was isolated from selfed progenies of the original *cuc* mutant line, whose genotype was *cuc1/cuc1 cuc2/+*, and this single mutant line was used as a tester line to confirm genotypes of the putative single mutant lines. Crosses between the tester and the single mutant from line 18 yielded no *cuc* seedlings in the F₂ generation, whereas crosses between the tester and the single mutant from line 20 yielded ~6.25% *cuc* seedlings, confirming that these single mutant lines were *cuc1* and *cuc2*, respectively.

Histological Analysis

For histological sections, tissues were fixed in 4% paraformaldehyde in phosphate buffer, pH 6.8, overnight at 4°C and dehydrated through an ethanol series. Embedding in Technovit 7100 (Heraeus Kulzer, Wehrheim, Germany) was performed according to the manufacturer's directions. Sections (3 to 5 μ m thick) were cut with a microtome, attached to slides, and stained with toluidine blue.

Clearing of embryos and seedlings was performed basically as de-

scribed by Yadegari et al. (1994). Siliques or seedlings were fixed overnight in ethanol-acetic acid (9:1) solution at room temperature. After rehydration in a graded ethanol series (90, 70, 50, and 30%) for 20 min each, siliques or seedlings were cleared with a chloral hydrate-glycerol-water solution (8 g of chloral hydrate, 1 mL of glycerol, and 2 mL of water). Cleared ovules were dissected from siliques before observation. In some cases, embryos were further dissected from ovules.

Scanning Electron Microscopy

Flowers were fixed, dehydrated, and critical point dried as described by Smyth et al. (1990). Flowers were then mounted on stubs and coated with gold in an ion sputter coater before observation.

Shoot Regeneration

Shoot regeneration was performed as described by Akama et al. (1992), with the following modifications. The concentration of kinetin in callus-inducing medium was 100 rather than 50 $\mu\text{g/L}$. The concentration of N^6 -(Δ^2 -isopentenyl)adenine in shoot-inducing medium was 0.5 mg/L rather than 5 mg/L.

DNA Isolation

Frozen plant tissues were ground and incubated for 1 hr at 55°C with 100 $\mu\text{g/mL}$ proteinase K, 100 mM Tris-HCl, pH 8, 100 mM EDTA, 250 mM NaCl, and 1% Sarkosyl. Samples were centrifuged at 5000g for 10 min, and the supernatants were placed in new tubes. DNAs were precipitated by the addition of 0.6 volumes of isopropanol. DNAs were pelleted by centrifugation at 8000g for 15 min, suspended in Tris-EDTA buffer, and purified by CsCl banding.

DNA Gel Blot Analysis

Two micrograms of genomic DNA was digested with restriction enzymes, electrophoresed on 1% agarose gel, and transferred to nylon membranes. Membranes were prehybridized for 2 hr at 55°C in a solution containing 6 \times SSC (1 \times SSC is 0.15 M NaCl, 0.015 M sodium citrate), 10 \times Denhardt's solution (1 \times Denhardt's solution is 0.02% Ficoll, 0.02% PVP, 0.02% BSA), 0.1% SDS, and 500 $\mu\text{g/mL}$ salmon sperm DNA and then hybridized with a radiolabeled *Tag1* or *Activator* (*Ac*) fragment overnight at 55°C. The *Tag1* fragment was a 1324-bp inner fragment of *Tag1* digested with EcoRI. The *Ac* fragment was a 904-bp inner fragment of *Ac* digested with both EcoRI and HindIII. Washing was performed twice for 15 min in 6 \times SSC and 0.1% SDS, twice for 15 min in 1 \times SSC and 0.1% SDS, and twice for 15 min in 0.1 \times SSC and 0.1% SDS at 55°C.

Cloning and Sequence Analysis of *CUC2*

With the amplified *Tag1* flanking region, a genomic library of the *Arabidopsis* (Columbia ecotype) in EMBL3 SP6/T7 (Clontech, Palo Alto, CA) was screened. Eleven clones were isolated from $\sim 7 \times 10^5$ plaques. Phage DNA was prepared and sequenced directly using a dye terminator cycle sequencing kit (Perkin-Elmer, Branchburg, NJ) according to the manufacturer's instructions. Synthetic primers were

used for sequencing. The insertion and footprints of *Tag1* were confirmed by direct sequencing of PCR products spanning the regions of interest. The GenBank, EMBL, and DDBJ accession number of *CUC2* is AB002560.

RNA Isolation

Frozen plant tissues (~ 5 g) were ground and homogenized in 27 mL of TLE solution (200 mM Tris, 100 mM LiCl, and 5 mM EDTA, pH 8.2), 3 mL of 10% SDS, and 10 mL of TLE-equilibrated phenol. After the addition of 10 mL of chloroform, the mixtures were homogenized and centrifuged at 8000g for 10 min. The aqueous phases were extracted twice with 20 mL of TLE-equilibrated phenol-chloroform and once with 20 mL of chloroform. RNAs were precipitated by the addition of one-third volumes of 8 M LiCl overnight at 4°C. RNAs were pelleted by centrifugation at 8000g for 20 min, suspended in 5 mL of water, and reprecipitated by the addition of one-third volumes of 8 M LiCl for 4 to 6 hr at 4°C. RNAs were repelleted by centrifugation and resuspended in 400 μL of water. After the addition of one-tenth volumes of 5 M NaCl, the suspensions were centrifuged at 14,000 rpm for 20 min to remove carbohydrates. The supernatants were transferred to new tubes, and RNAs were ethanol precipitated and resuspended in 100 μL of Tris-EDTA buffer. The RNA concentrations were determined by UV absorbance.

Inflorescence stems, mature rosette leaves, buds from stages 0 to 12 (Smyth et al., 1990), open flowers, young siliques (containing zygotes to torpedo-stage embryos), and old siliques (containing torpedo-stage to mature embryos) were harvested from 1-month-old plants grown on soil. Aerial and root tissues were harvested from seedlings grown on Murashige and Skoog plates under continuous light for 7 days.

RNA Gel Blot Analysis

Poly(A)⁺ RNAs were isolated with oligo(dT)-latex (Japan Synthetic Rubber, Tokyo), according to the manufacturer's instructions. Five micrograms of poly(A)⁺ RNAs was electrophoresed on 1% agarose gel containing 2.2 M formaldehyde and transferred to nylon membranes. Membranes were prehybridized for 4 hr at 42°C in a solution containing 50% formamide, 5 \times Denhardt's solution, 5 \times SSC, 50 mM NaH₂PO₄, pH 5.95, and 250 $\mu\text{g/mL}$ salmon sperm DNA. Hybridization was performed overnight at 42°C in a solution containing 10% dextran sulfate, 50% formamide, 1 \times Denhardt's solution, 4 \times SSC, 50 mM NaH₂PO₄, pH 5.95, and radiolabeled probes. To specifically detect *CUC2* mRNA, a DNA fragment corresponding to the third exon of *CUC2* was used as a probe. After hybridization, membranes were washed once for 30 min in 6 \times SSC and 0.1% SDS, once for 30 min in 1 \times SSC and 0.1% SDS, and twice for 30 min in 0.1 \times SSC and 0.1% SDS at 55°C.

PCR Conditions

PCR conditions are as follows. PCR mixtures (10 μL) contained 1 \times PCR buffer (Perkin-Elmer or Takara Shuzo, Ohtsu, Japan), 250 μM dATP, dTTP, dGTP, and dCTP, 1 μM primers, 2% formamide, 2.5 units of Taq DNA polymerase (Perkin-Elmer or Takara Shuzo), and 1 μL of template. The PCR program was as follows: preheating for 1.3 min at 92°C, 35 cycles of heating for 0.8 min at 92°C, annealing for 2 min at 55°C, and extension for 3 min at 72°C, with a final extension

for 10 min at 72°C. In the case of inverse PCR and internal control of reverse transcriptase-PCR (RT-PCR), formamide was not added to the PCR mixture and annealings were performed at 50°C.

RT-PCR

RT-PCR was performed using the RNA map kit (GenHunter, Brookline, MA). Total RNA (1.0 µg) was incubated for 5 min at 65°C in a 9-µL solution containing 2 µL of 5 × RT buffer, 0.8 µL of deoxynucleotide triphosphates (2.5 mM each), and 1.25 µL of oligo(dT) primer (5'-TTAAGCTTTTTTTTTTTTTTTTTT-3' [10 µM]) and cooled to 37°C. Then, 1.0 µL of Moloney murine leukemia virus RT (100 units per µL) was added, and reactions were performed for 1 hr at 37°C. Parts of these reactions were used as templates for PCR. *CUC2* mRNA was detected with the primers CUP3 (5'-CAGCCAATATCTCCACCGGG-3'; located in the first exon) and CUP11 (5'-GGAGAGGTGGGAGTGAGACGGA-3'; located in the third exon). As a positive internal control, *ACT8* was used (An et al., 1996). Specific primers for detection of *ACT8* mRNA were 5'-ATGAAGATTAAGGTCGTGGCA-3' and 5'-TCCGAGTTTGAAGAGGCTAC-3'.

ACKNOWLEDGMENTS

We thank Drs. Nigel M. Crawford and Caroline Dean for providing the *chl1-6* seeds and the *Tag1* and *Ac* DNA fragments. We also thank Drs. Tsuneyoshi Kuroiwa (University of Tokyo) and Makoto Hayashi (Institute of Physical and Chemical Research, Wako, Japan) for technical help with the histological analysis. We acknowledge the Arabidopsis Biological Resource Center (Ohio State University, Columbus) for providing the CS3078 mapping line. This work was supported in part by a Grant-in-Aid for Scientific Research on Priority Areas (Molecular Basis of Flexible Organ Plans in Plants, Nos. 07270212, 08262212, and 08640825).

Received December 2, 1996; accepted March 24, 1997.

REFERENCES

- Akama, K., Shiraishi, H., Ohta, S., Nakamura, K., Okada, K., and Shimura, Y. (1992). Efficient transformation of *Arabidopsis thaliana*: Comparison of the efficiencies with various organs, plant ecotypes and *Agrobacterium* strains. *Plant Cell Rep.* **12**, 7–11.
- An, Y.-Q., McDowell, J.M., Huang, S., McKinney, E.C., Chambliss, S., and Meagher, R.B. (1996). Strong, constitutive expression of the *Arabidopsis ACT2/ACT8* actin subclass in vegetative tissues. *Plant J.* **10**, 107–121.
- Barton, M.K., and Poethig, R.S. (1993). Formation of the shoot apical meristem in *Arabidopsis thaliana*: An analysis of development in the wild type and in the *shoot meristemless* mutant. *Development* **119**, 823–831.
- Bell, C.J., and Ecker, J.R. (1994). Assignment of 30 microsatellite loci to the linkage map of *Arabidopsis*. *Genomics* **19**, 137–144.
- Bowman, J.L., Alvarez, J., Weigel, D., Meyerowitz, E.M., and Smyth, D.R. (1993). Control of flower development in *Arabidopsis thaliana* by *APETALA1* and interacting genes. *Development* **119**, 721–743.
- Coen, E.S., and Meyerowitz, E.M. (1991). The war of the whorls: Genetic interactions controlling flower development. *Nature* **353**, 31–37.
- Fukaki, H., Fujisawa, H., and Tasaka, M. (1996a). Gravitropic response of inflorescence stems in *Arabidopsis thaliana*. *Plant Physiol.* **110**, 933–943.
- Fukaki, H., Fujisawa, H., and Tasaka, M. (1996b). *SGR1*, *SGR2*, and *SGR3*: Novel genetic loci involved in shoot gravitropism in *Arabidopsis thaliana*. *Plant Physiol.* **110**, 945–955.
- Jürgens, G. (1995). Axis formation in plant embryogenesis: Cues and clues. *Cell* **81**, 467–470.
- Jürgens, G., Torres Ruiz, R.A., and Berleth, T. (1994a). Embryonic pattern formation in flowering plants. *Annu. Rev. Genet.* **28**, 351–371.
- Jürgens, G., Torres Ruiz, R.A., Laux, T., Mayer, U., and Berleth, T. (1994b). Early events in apical-basal pattern formation in *Arabidopsis*. In *Plant Molecular Biology*, G. Coruzzi and P. Puigdomènech, eds (Berlin: Springer-Verlag), pp. 95–103.
- Kempin, S.A., Savidge, B., and Yanofsky, M.F. (1995). Molecular basis of the *cauliflower* phenotype in *Arabidopsis*. *Science* **267**, 522–525.
- Konieczny, A., and Ausubel, F.M. (1993). A procedure for mapping *Arabidopsis* mutations using co-dominant ecotype-specific PCR-based markers. *Plant J.* **4**, 403–410.
- Laux, T., Mayer, K.F.X., Berger, J., and Jürgens, G. (1996). The *WUSCHEL* gene is required for shoot and floral meristem integrity in *Arabidopsis*. *Development* **122**, 87–96.
- Long, J.A., Moan, E.I., Medford, J.I., and Barton, M.K. (1996). A member of the KNOTTED class of homeodomain proteins encoded by the *STM* gene of *Arabidopsis*. *Nature* **379**, 66–69.
- Mandel, M.A., Gustafson-Brown, C., Savidge, B., and Yanofsky, M.F. (1992). Molecular characterization of the *Arabidopsis* floral homeotic gene *APETALA1*. *Nature* **360**, 273–277.
- Mansfield, S.G., and Briarty, L.G. (1991). Early embryogenesis in *Arabidopsis thaliana*. II. The developing embryo. *Can. J. Bot.* **69**, 461–476.
- Mayer, U., Torres Ruiz, R.A., Berleth, T., Miséra, S., and Jürgens, G. (1991). Mutations affecting body organization in the *Arabidopsis* embryo. *Nature* **353**, 402–407.
- Mayer, U., Berleth, T., Torres Ruiz, R.A., Miséra, S., and Jürgens, G. (1993). Pattern formation during *Arabidopsis* embryo development. In *Cellular Communication in Plants*, R.M. Amasino, ed (New York: Plenum Press), pp. 93–98.
- Medford, J.I. (1992). Vegetative apical meristems. *Plant Cell* **4**, 1029–1039.
- Pickett, F.B., and Meeks-Wagner, D.R. (1995). Seeing double: Appreciating genetic redundancy. *Plant Cell* **7**, 1347–1356.
- Smyth, D.R., Bowman, J.L., and Meyerowitz, E.M. (1990). Early flower development in *Arabidopsis*. *Plant Cell* **2**, 755–767.
- Souer, E., Van Houwelingen, A., Kloos, D., Mol, J., and Koes, R. (1996). The *no apical meristem* gene of petunia is required for pattern formation in embryos and flowers and is expressed at meristem and primordia boundaries. *Cell* **85**, 159–170.
- Sussex, I.M. (1989). Developmental programming of the shoot meristem. *Cell* **56**, 225–229.

- Thomas, J.H.** (1993). Thinking about genetic redundancy. *Trends Genet.* **9**, 395–399.
- Tsay, Y.-F., Frank, M.J., Page, T., Dean, C., and Crawford, N.M.** (1993). Identification of a mobile endogenous transposon in *Arabidopsis thaliana*. *Science* **260**, 342–344.
- Van der Krol, A.R., and Chua, N.-H.** (1993). Flower development in petunia. *Plant Cell* **5**, 1195–1203.
- Weigel, D., and Meyerowitz, E.M.** (1994). The ABCs of floral homeotic genes. *Cell* **78**, 203–209.
- West, M.A.L., and Harada, J.J.** (1993). Embryogenesis in higher plants: An overview. *Plant Cell* **5**, 1361–1369.
- Yadegari, R., de Paiva, G.R., Laux, T., Koltunow, A.M., Apuya, N., Zimmerman, J.L., Fischer, R.L., Harada, J.J., and Goldberg, R.B.** (1994). Cell differentiation and morphogenesis are uncoupled in *Arabidopsis raspberry* embryos. *Plant Cell* **6**, 1713–1729.